

Elastic manifolds in disordered environments: energy statistics

K. P. J. KYTÖLÄ¹, E. T. SEPPÄLÄ² and M. J. ALAVA¹

¹ *Helsinki University of Technology, Laboratory of Physics, P.O.Box 1100, FIN-02015 HUT, Finland*

² *Lawrence Livermore National Laboratory, 7000 East Avenue, L-415, Livermore, CA 94550, U.S.A.*

PACS. 05.70.Np – Interface and surface thermodynamics.

PACS. 75.50.Lk – Spin glasses and other random magnets.

PACS. 68.35.Ct – Interface structure and roughness.

Abstract. – The energy of an elastic manifold in a random landscape at $T = 0$ is shown numerically to obey a probability distribution that depends on size of the box it is put into. If the extent of the spatial fluctuations of the manifold is much less than that of the system, a cross-over takes place to the Gumbel-distribution of extreme statistics. If they are comparable, the distributions have non-Gaussian, stretched exponential tails. The low-energy and high-energy stretching exponents are roughly independent of the internal dimension and the fluctuation degrees of freedom.

The statistical mechanics of elastic objects or manifolds changes in the presence of disorder, since temperature becomes irrelevant as a scaling variable. The statistical properties are determined by the competition of elasticity and randomness. Examples of systems where this happens are domain walls (DW) in random magnets and flux lines in superconductors [1, 2, 3]. At the zero temperature “fixed point” in the renormalization group language, the geometry of the object becomes critical. The fluctuations are self-affine below the upper critical dimension of the Hamiltonian. This upper critical dimension may or may not have a finite value depending on the dimensionality of the possible fluctuations. Examples are provided by the one-dimensional directed polymer (DP) in $n \geq 1$ fluctuation dimensions, which has a low-temperature phase for which $n_c = \infty$ [2]. Another case is given by D internal-dimensional random manifolds in $d = (D + n)$ dimensions, where $n = 1$, which are known to have the upper critical dimension $D_c = 4$ [3].

The criticality of elastic manifolds is manifested by the distribution of energies, $P(E)$, which is not a Gaussian. This was shown by extensive simulations of directed polymers in $d = (D + n) = (1 + 1)$ and $(1+2)$ dimensions (d is the total, embedding space dimension of a system) [4]. In these simulations a DP was let to minimize its energy by keeping one end fixed, and letting the other one wander freely. The outcome is that for energies smaller than the average, $E_- \ll \langle E \rangle$, the distribution $P(E) \sim \exp[-|E|^{\eta_-}]$, *i.e.*, *stretched exponential*. Note that the distribution is normalized in such a way that the average of E is zero and its variance

or standard deviation equals unity. Similarly for $E_+ \gg \langle E \rangle$ one obtains a stretching exponent η_+ . These stretching exponents are below the Gaussian $\eta = 2$ value for small energies and above it for large ones, and their numerical values are rather insensitive to whether $n = 1$ or 2.

What has not been addressed so far is how exactly the scaling function, $P(E)$, depends on the set of boundary conditions imposed on the manifold and the dimensions n and D . One reason is that computing $P(E)$ is naturally a rather formidable task. One rare analogy is provided by the (1+1)-dimensional Kardar-Parisi-Zhang-equation (KPZ) [5], in the form of the asymmetric exclusion process (ASEP). This system is governed by the “strong coupling fixed point” of the KPZ interface growth. Approaches based on a generalized free energy by Derrida and Lebowitz [6] and on mapping the problem to random matrix theory (by Prähofer and Spohn [7]) have succeeded in deriving analytically the non-Gaussian scaling functions. This is true for the velocity fluctuations or height fluctuations in the two respective cases but only in the *steady-state* of the growth, that is when the correlation length exactly equals the system size. In the KPZ case in (1+1)-dimensions one can also resort to scaling arguments for the extremal properties of the interface statistics, predicting $\eta_- = 3/2$ [8].

In this Letter we show that the problem of the shape of the probability distribution $P(E)$ is actually continuously dependent on a natural boundary condition, namely the transverse height of the system. It is also, on the other hand, rather independent of the dimensionality. The continuum of exponents η_+ , η_- for $P(E)$ results from the cross-over from a Gaussian distribution (when the height of the system is limited to below the natural roughness or geometrical fluctuations and hence reflects Poissonian statistics) to the Gumbel function of extreme statistics [9,10] when the transverse height of the system is let to increase to infinity. It turns out to be so that the variation of the η_- , η_+ is related to so-called penultimate extremal distributions, the scaling of an extremal quantity from samples with a *finite* number of independent variables.

There remain several open questions that we return to in the summary. Recall that the energy of a DP relates to the first arrival time of a KPZ interface to a fixed height (a related problem but not quite the same is the maximal height of an interface with a given average height [11]). Hence varying the transverse height thus equals moving between the stationary state and an initial transient. The former can be accessed via the large deviation and random matrix formalisms [6,7]. In our numerical simulations we have varied both the internal dimension of the system D , which gets values from one to three, and the fluctuation degree of freedom n , which gets the same values. We are for algorithmic reasons restricted to cases, where whenever $D > 1$ n has to have a value of unity, and vice versa.

The geometric fluctuations of elastic manifolds can be measured by the two-point correlation function or by mean-square fluctuations. These define the roughness exponent ζ , *e.g.* as $w^2 = \langle [z(\mathbf{x}) - \overline{z(\mathbf{x})}]^2 \rangle \sim L^{2\zeta}$, where L is the linear size of the system, $z(\mathbf{x})$ is the manifold’s height and \mathbf{x} is the D dimensional internal coordinate of the manifold. For the ground state or free energy fluctuations around the disorder-averaged mean one has that $\Delta E = \langle (E - \langle E \rangle)^2 \rangle^{1/2} \sim L^\theta$, where $\theta = 2\zeta + D - 2$ [12]. The ground state energy is a quenched random variable and it behaves as $E \sim AL^D + BL^\theta$. Thus normal equilibrium behavior is modified, and the (free) energy develops non-analytic corrections. In a renormalization picture the energy fluctuation exponent θ arises naturally. We concentrate on random-bond disorder, which means that the random-potential in the energy Hamiltonian is delta-point correlated, although the results should be applicable to other types of short-range correlated randomness, too. At low temperatures in (1+1) dimensions, due to the equivalence of the directed polymer in random media [5,2] to the KPZ equation, the exact roughness expo-

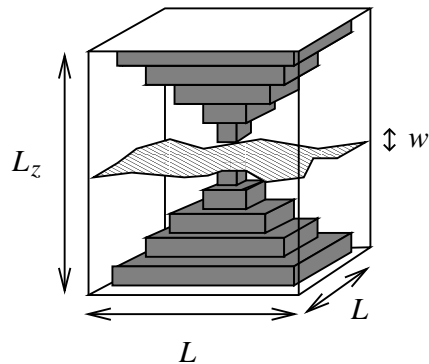


Fig. 1 – A sketch of $(D + n) = (2 + 1)$ dimensional manifold in a system, whose lateral size, perpendicular to the average normal of the surface, is $L_x = L_y = L$ and transverse height, parallel to the average surface normal, is L_z . The width, root-mean-square fluctuation, of the surface is w . When the manifold is pinned in the center of the system, the “cone” geometry is used. In that case the area where the surface is not allowed to pass through is depicted with gray.

ment is $\zeta = 2/3$, with RB disorder [5,2,13]. In higher D dimensions functional renormalization group calculations give $\zeta \simeq 0.208(4 - D)$ [3]. The $(1 + n)$ dimensional directed polymers with $n > 1$ have roughness values $\zeta = 0.62$ and $\zeta = 0.59$, when $n = 2$ and $n = 3$, respectively (see *e.g.* [2]).

For numerical calculations, when $D \geq 1$, the optimization of the Hamiltonian of a manifold in random bond environment (which is equivalent with domain wall in random-bond Ising magnet) maps into the minimum cut-maximum flow problem of combinatorial optimization [14,15]. The simulations of $D = 1$, $n \geq 1$ directed-polymers are done using the standard transfer-matrix (TM) method [16]. Here we impose two different type of boundary conditions in the transverse height direction of the system, *i.e.*, in the direction of the average normal of the D dimensional manifold. The manifold is fixed in a single valley by pinning it at certain coordinate, or let to float freely, so that the mean height can vary in a box defined by the system height L_z . For DP’s the pinning follows in the TM simulations from having one end fixed and the other one free. For $D > 1$ manifolds we construct a new way to create a “one valley” case since the same trick as for DP’s to fix the manifold at a fixed height does not work, for dimensional reasons. Our pinning method is illustrated in the $(2+1)$ -dimensional case in Fig. 1 and is also in the simulations extended to $(3+1)$ -dimensions.

We have shown earlier that the average manifold energy develops a logarithmic dependence on L_z [17,18] due to extremal statistics. Since the width of a directed manifold grows as L^ζ it is expected that there is a number N_z of quasi-independent valleys in the energy landscape [19,20,21], proportional to $N_z \sim L_z/L^\zeta$. N_z thus presents a scaling parameter, and the Gumbel limit is obtained for L fixed in the limit $L_z \rightarrow \infty$, $N_z \rightarrow \infty$. Hence the logarithmic dependence on L_z results straightforwardly from extreme statistics. We first study $P(E)$ in the case of the “one valley” systems, $N_z = 1$, and then in the case when L_z or N_z is varied.

Figs. 2(a) and 2(b) demonstrate the phenomenology of $P(E)$ for various dimensionalities in the “one valley” case. We see that the scaled probability distributions are rather independent of D and n though the actual scaling exponents ζ and θ vary greatly. This is most striking if one considers the integrated distribution [Fig. 2(b)]. However, there we concentrate in the part of the distribution, which is close to mean, and as the actual shape is usually close to Gaussian

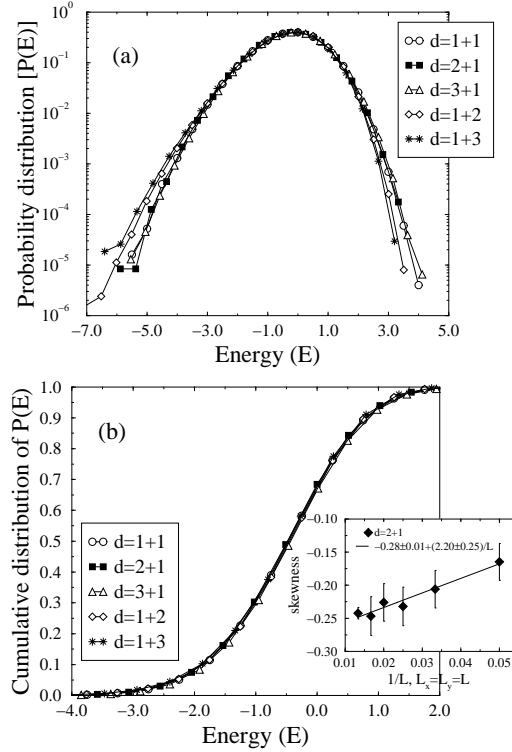


Fig. 2 – (a) The normalized energy distributions, $\langle E \rangle = 0$ and $\Delta E = 1$, for manifolds with various D and n in a “single valley” case, *i.e.*, pinned when $D = 1$ or using “cone” geometry when $D > 1$ ($L_z = L$). The number of random configurations $N = 5 \times 10^5$ and the lateral size of the system $L = 100$ for $(D + n) = (1 + 1)$. Similarly $N = 2.3 \times 10^5$ and $L^2 = 75^2$ for $(D + n) = (2 + 1)$; $N = 3.2 \times 10^5$ and $L^3 = 25^3$ for $(D + n) = (3 + 1)$; $N = 2.5 \times 10^6$ and $L = 70$ for $(D + n) = (1 + 2)$; $N = 5.1 \times 10^5$ and $L = 50$ for $(D + n) = (1 + 3)$. (b) Cumulative distribution $\int P(E) dE$ for the same data as in (a). The inset shows skewness, $\langle [(E - \langle E \rangle) / \Delta E]^3 \rangle$, versus lateral size, $L_x = L_y = L$, for $(D + n) = (2 + 1)$. The “cone” geometry is used in the transverse direction. The solid line is the least-squares-fit to the data leading to a value of -0.28 ± 0.01 . The number of random configurations $N = 10^4$ for all the other L except $L = 75$ for which the data is the same as in (a) and (b).

the differences in the tails cannot even be visible. One of the features of the behavior of $P(E)$ is that while the skewness, *i.e.*, 3rd moment, $\sigma_3 = \langle [(E - \langle E \rangle) / \Delta E]^3 \rangle$, is L -dependent the tail exponents are much less sensitive to the system size. The inset demonstrates an extrapolation of skewness for $(2+1)$ -dimensions, and we obtain $\sigma_3 = -0.28 \pm 0.01$.

Let us now consider what happens as a function of $N_z = L_z/w$. If $N_z \ll 1$ the interface is confined to a “box” which is smaller than the expected roughness, thus criticality is destroyed and $P(E)$ becomes a Gaussian. If N_z is increased (by L_z) the outcome is depicted in Fig. 3(a). For all the varying dimensionalities we obtain a steady but very slow cross-over of $P(E)$ towards a fast decay on the side of large energies ($E \gg \langle E \rangle$) and a slower one on the other side. In the asymptotic limit one expects that the Gumbel distribution is found, which has the form (in scaled units) $P_{Gumbel} \sim \exp(E - \exp E)$. The convergence is an example of penultimate extremal distributions. For N_z finite the extremal probability-density-function (PDF) is given by a form which has a point-wise limit in the asymptotic distribution [22, 23], but may

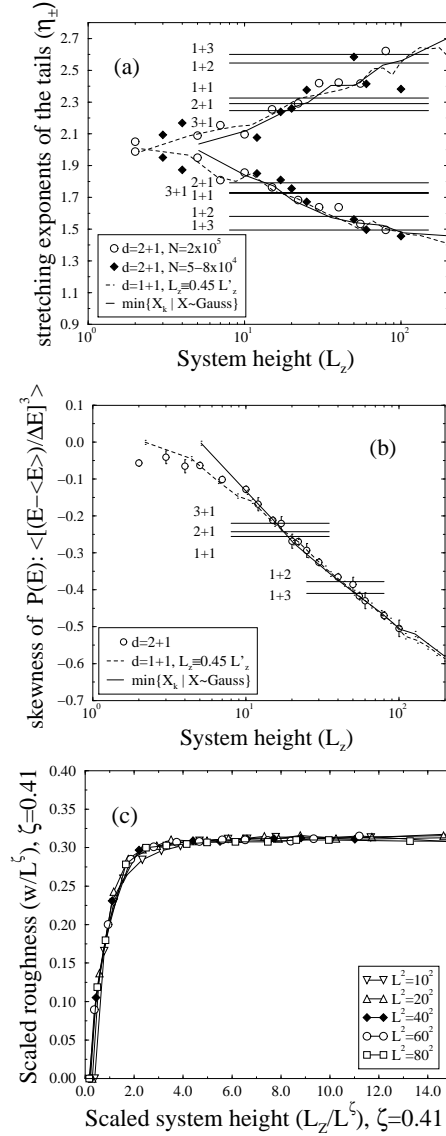


Fig. 3 – (a) Stretching exponents, η_- and η_+ , of the left and right-hand tails, respectively, of the energy distributions, $\exp\{-|(E - \langle E \rangle) / \Delta E|^{\eta_{\pm}}\}$, for $(D + n) = (1 + 1)$ and $(2 + 1)$ versus the system height L_z in unpinned (and non-cone-geometry) cases. Open circles and filled diamonds are from $(2 + 1)$ dimensional data. The first one has $N = 2 \times 10^5$, while the latter has $N = 5 - 8 \times 10^4$. For both data set $L_x = L_y = L = 40$. $(D + n) = (1 + 1)$ is plotted as a dashed line. In that case $L = 100$. In order to show the similarity of the trends with $(D + n) = (2 + 1)$ L_z for $(1 + 1)$ are scaled by a factor of 0.45. The solid line shows the stretching exponent for the distribution of the minimum of several Gaussian distributions $\min\{X_k | X \sim \text{Gauss}, k = 1, 2, \dots, N_G\}$ versus the number of Gaussian distributions N_G . In that case the x -axis is scaled so that $N_G = 5.1L_z$. The horizontal lines show the stretching exponent values η_{\pm} of the distributions plotted in Fig. 2(a). (b) The skewness values of the same distributions as in (a). For $(D + n) = (2 + 1)$ only the data with better statistics $N = 2 \times 10^5$ is shown. For $(D + n) = (1 + 1)$ and for the Gaussian case we use the same x -axis scalings as in (a). The horizontal lines show the skewness values of the distributions plotted in Fig. 2(a). (c) The scaled roughness w/L^ζ vs. scaled system height L_z/L^ζ , where $\zeta = 0.41$, for $(D + n) = (2 + 1)$ and various lateral lengths of the system $L_x = L_y = L = 10, 20, 40, 60$, and 80 . The number of realizations varies from $N = 1000$ for $L = 10$ to $N = 600$ for $L = 80$.

TABLE I – The skewness σ_3 and stretching exponent values η_- and η_+ of the distributions plotted in Fig. 2(a).

D	n	σ_3	η_-	η_+
3	1	-0.22 ± 0.01	1.73 ± 0.10	2.25 ± 0.10
2	1	-0.24 ± 0.01	1.79 ± 0.10	2.29 ± 0.10
1	1	-0.26 ± 0.01	1.72 ± 0.10	2.33 ± 0.10
1	2	-0.38 ± 0.01	1.58 ± 0.10	2.55 ± 0.10
1	3	-0.41 ± 0.01	1.49 ± 0.10	2.60 ± 0.10

e.g. exhibit stretched exponential tails, such that the behavior of the exponents is in agreement with the convergence to the asymptotic. Thus η_- increases, and η_+ decreases. Penultimate distributions depend on many factors and can resemble more the other two asymptotic forms (than the Gumbel) [23], and the convergence can be very slow.

Next, one can pose the question: is the one-valley ensemble (with appropriate boundary conditions) equivalent to what one gets in the limit $N_z \simeq 1$, *i.e.*, are the P 's the same? This is not a trivial one since the N_z -ensemble is “grand-canonical”, the number of “valleys” is not defined in any sample except in the average sense (recall also the KPZ-growth analogy for DP's). Our numerical results imply that this is roughly the case. We also show that the convergence of the exponents is reproduced [as depicted in Fig. 3(a)] by a simple Gaussian model. We mimic a single-valley distribution by picking the minimum out of a small number of independent-and-identically-distributed Gaussian variables. Then N_z is varied and the smallest of N_z such ones is chosen. This gives rise to the last set of data in the figure, and as can be seen it reproduces the manifold results qualitatively and almost quantitatively. This analogy reinforces the picture of independent valleys and N_z as a scaling parameter.

One may thus consider the tail exponents η_- and η_+ to be “hyper-universal” as the actual values depend mostly on the ensemble and, within the numerical accuracy, almost not at all on the dimensionality. The actual values of the tail exponents and the skewnesses are reported in Table I. However the actual scaling functions of $P(E)$ are not quite the same, as is demonstrated by Fig. 3(b) where the skewnesses of the scaled $P(E)$'s are shown for “single valley” ensembles, and compared to the skewness for various N_z or L_z . As expected from the Gaussian-to-Gumbel cross-over the skewnesses vary continuously. We finish with Fig. 3(c), which shows reasonably conclusively in (2+1)-dimensions, the average roughness, another critical property, is little if at all affected by the ensemble. What the figure demonstrates is the insensitivity of the amplitude $a(N_z)$ in $w = a(N_z)L^\zeta$, $\zeta = 0.41$ to N_z once $N_z > 1$. This is in contrast to the average energy [17].

To conclude we have here studied the statistics of the ground state energy of critical elastic manifolds in random systems. These are the first numerical calculations of the energy distribution, when $D > 1$. We show that the scaling function of the energy is a continuous function of the external control parameter, the system “thickness” N_z . Thus the properties of the tails of $P(E)$ depend crucially on such details, but not so much on dimensionality or in other words the actual scaling exponents of the problem. One should note that the expected variation of η_- , η_+ is typically logarithmic in N_z using usual convergence rates of penultimate distribution extreme statistics. Therefore, such exponents have rather “arbitrary” values.

There are three open problems that we can outline. First, is it indeed mostly a mathematical accident that *e.g.* $\eta_- \sim 1.5 \dots 1.7$ for all D and n in the single-valley ensembles? The existence of such tails tells that all critical manifolds might share some general properties with

the KPZ-equation related systems that can be treated on an analytical basis. In particular the free energy or large deviation functional could be in such a case non-local. Second, it would be interesting (but numerically extremely hard) to look at $T > 0$ the free energy distribution in the general case, except say for the $(1 + 1)$ dimensional directed polymers, which is relatively easy and has been studied in the literature [4]. Third, one particular example of a “critical manifold” is given by random field Ising magnets (RFIM) at the bulk phase transition, since here one can map the problem to RB domain walls in $(D + 1)$ dimensions. Our results imply that the distribution of the ground state energy should prove to be an interesting quantity, in three (3D) and four dimensions. This is so in particular since there is in the much-debated 3D case substantial numerical evidence that the aspect ratio of the system will affect the domain structure (and thus perhaps the energy distribution).

* * *

This work has been supported by the Academy of Finland’s Centre of Excellence Programme. It was also performed under the auspices of the U.S. Dept. of Energy at the University of California/Lawrence Livermore National Laboratory under contract no. W-7405-Eng-48 (ETS). MJA would like to thank professors S. Coles and L. de Haan for correspondence on extremal statistics.

REFERENCES

- [1] BLATTER G., FEIGEL’MAN M. V., GESHKENBEIN V. B., LARKIN A. I. and VINOKUR V. M., *Rev. Mod. Phys.*, **66** (1994) 1125.
- [2] HALPIN-HEALY T. and ZHANG Y.-C., *Phys. Rep.*, **254** (1995) 215.
- [3] FISHER D., *Phys. Rev. Lett.*, **56** (1986) 1964.
- [4] KIM J. M., MOORE M. A. and BRAY A. J., *Phys. Rev. A*, **44** (1991) 2345.
- [5] KARDAR M., PARISI G. and ZHANG Y.-C., *Phys. Rev. Lett.*, **56** (1986) 889.
- [6] DERRIDA B. and LEBOWITZ J., *Phys. Rev. Lett.*, **80** (1998) 209.
- [7] PRÄHOFER M. and SPOHN H., *Phys. Rev. Lett.*, **84** (2000) 4882.
- [8] The example is polynuclear growth in $d = 2$, see BEN-NAIM E., BISHOP A. R., DARUKA I. and KRAPIVSKY P. L., *J. Phys. A*, **31** (1998) 4001.
- [9] GALAMBOS J., *The Asymptotic Theory of Extreme Order Statistics* (John Wiley & Sons, New York) 1978.
- [10] BOUCHAUD J.-P. and MÉZARD M., *J. Phys. A*, **30** (1997) 7997.
- [11] RAYCHAUDHURI S., CRANSTON, M., PRZYBYLA, C. and SHAPIR. Y., *Phys. Rev. Lett.*, **87** (2001) 136101.
- [12] HUSE D. A. and HENLEY C. L., *Phys. Rev. Lett.*, **54** (1985) 2708.
- [13] BARABÁSI A.-L. and STANLEY H. E., *Fractal concepts in surface growth* (Cambridge University Press, Cambridge) 1995.
- [14] GOLDBERG A. V. and TARJAN R. E., *J. Assoc. Comput. Mach.*, **35** (1988) 921.
- [15] ALAVA M., DUXBURY P., MOUKARZEL C. and RIEGER H., *Phase Transitions and Critical Phenomena*, edited by DOMB C. and LEBOWITZ J. L., Vol. **18** (Academic Press, London) 2001.
- [16] KARDAR M. and ZHANG Y.-C., *Phys. Rev. Lett.*, **58** (1987) 2087.
- [17] SEPPÄLÄ E. T., ALAVA M. J. and DUXBURY P. M., *Phys. Rev. E*, **63** (2001) 066110.
- [18] SEPPÄLÄ E. T. and ALAVA M. J., *Eur. Phys. J. B*, **21** (2001) 407.
- [19] MÉZARD M., *J. Phys. France*, **51** (1990) 1831.
- [20] HWA T. and FISHER D. S., *Phys. Rev. B*, **49** (1994) 3136.
- [21] SEPPÄLÄ E. T. and ALAVA M. J., *Phys. Rev. Lett.*, **84** (2000) 3982.
- [22] RESNICK S., *Extreme Values, Regular Variation, and Point Processes* (Springer, New York)

1987, sect. 2.4; REISS R. D. and THOMAS M., *Statistical Analysis of Extreme Values* (Birkhäuser, Basel) 2001, sect. 6.

- [23] GOMES M. I., *Comput. Stat. Data Anal.*, **4** (1986) 257; COHEN J. P., *Adv. Appl. Prob.*, **14** (1982) 324.